

Influencing Factors of Load Carrying Capacity and Cooperative Work Laws of Metro Uplift Piles

Bo Liu^{1,*}, Haoran Li¹ and Shuya Liu²

¹Structural Health Monitoring and Control Institute, Shijiazhuang Tiedao University, Shijiazhuang, 050043, China

²Shenzhen Metro Group Co., Ltd., Shenzhen, 518026, China

*Corresponding Author: Bo Liu. Email: liub33851809@163.com.

Received: 28 February 2019; Accepted: 23 May 2019

Abstract: The buoyancy of groundwater can reduce the foundation bearing capacity and cause the metro tunnels to float as a whole, which threatens the safety of structures seriously. Therefore, uplift piles are set up to improve the structural stability. In this paper, FLAC3D software is used to establish the calculation models of pile foundation. The bearing failure process of uplift piles was simulated to study the influencing factors on single pile load bearing capacity as well as the cooperative work laws of pile groups. The load-displacement curves of pile top under different length-diameter ratios, pile-soil interface characteristics and pile types are obtained, respectively. The results showed that, increasing the length-diameter ratio and the pile-soil interface roughness properly can improve the bearing capacity of uplift piles. Besides, changing the shapes of constant pile section can also improve it, which has the most significant effect concerning of saving material cost. In the loading process of pile groups, the ultimate bearing capacity of corner pile is the biggest, the side pile is the next, and the center pile is the smallest. The deformation characteristics of pile top are as follows: the center pile is the biggest, the side pile is the next, and corner pile is the smallest. Combined with the results, the uplift resistance of group piles can be enhanced pertinently, and the conclusions provide guidance for the design and construction of uplift piles in the actual engineer.

Keywords: Uplift pile; length-diameter ratio; ultimate bearing capacity; cooperative work

1 Introduction

In recent years, underground space has been gradually developed, and the underground engineering such as subway and underground garage, etc. has been flourished. However, for areas with abundant groundwater resources and large permeability coefficient of soil, the water will infiltrate and soften the soil, causing the structure to float as a whole, and the problem is prominent with the increasing embedment depth of the foundation. Therefore, structural anti-floating has gradually becoming a new focus that affects the safety and durability of underground structures. Compared with various anti-floating measures, structure counterweight method is limited, especially for the projects with high water level and deep foundation, so



This work is licensed under a Creative Commons Attribution 4.0 International License, which permits unrestricted use, distribution, and reproduction in any medium, provided the original work is properly cited.

the uplift pile is extensively used for its high bearing capacity in the engineer. Researching on the anti-floating problems of underground structures, designing the uplift piles reasonably to improve the structural pullout behaviors are very important to ensure the safety of construction and the subway operation.

At present, it is in the initial or deepening stage with less research experience, and the results of uplift piles are mainly from three aspects: theoretical analysis, experimental research and numerical simulation. Combining with the nonlinear interface elements, Wang et al. [1] established a pile-soil mechanics model which was fully considered the Poisson effect of uplift piles derived from the Mindlin solution in elastic mechanics, and the side friction resistance was calculated accurately. Concerning of length-diameter ratio, surface characteristics of uplift piles and soil properties, Chattopadhyay et al. [2] proposed an analytical method for predicting the bearing capacity of uplift piles embedded in sand. Zhang et al. [3] simulated the interaction between pile-soil interface using the softening model and hyperbolic model. Based on these two models, two simple nonlinear analysis methods were proposed to study the load-displacement response of single uplift pile under the load. Alawneh [4] presented a load-displacement response method of uplift piles embedded in cohesive soil, and the hyperbolic formula is used to fit the transfer curve of nonlinear loads.

Because of the complexity of the bearing mechanism of uplift piles, scholars conducted numerous laboratory and field tests on the basis of theoretical analysis, and the results of experiments and theory research were compared together. Chen et al. [5,6] carried out lots of indoor model tests to study the compressive piles and uplift piles with the length-diameter ratio over 40 in layered soil and sand, respectively. By monitoring the strain resistances on pile surface, the deformation of piles embedded in different depths was obtained during the uplift loading process, and the distribution characteristics of side friction were also analyzed. Das et al. [7,8] neglected the pile weight to study the relativity between the bearing capacity and the side friction of uplift piles. The results showed that the decrease of bearing capacity is related to the friction angle of soil. Gaaver [9] applied uplift loads on single uplift pile and group piles in cohesionless soil. It was found that the performance of group piles mainly depended on the embedded depth, diameter ratio and the properties of soil, and the group efficiency decreased as the ratio of buried depth to diameter increased. Madhusudan Reddy et al. [10] analyzed the deformation characteristics of single pile under the uplift and lateral loads. Based on the material and dimension of prototype piles, the indoor model test was carried out according to the scaled standard. The results showed that the variation in load-deflection curves were nonlinear under the independent uplift and lateral loads. Besides, Eswar et al. [11] analyzed the bearing capacity of vertical and inclined piles by indoor tests. An empirical formula is obtained which provided a new idea for studying the uplift pile behaviors.

For model tests, models are required to establish similarly to the engineering situation, which will consume much of time and money. While, the computer simulation software can simulate the real situation of the engineering, which is easy to operate and costs less. For these reasons, the numerical simulation technology is extensively used in the research. Faizi et al. [12–14] used ABAQUS software to analyze the uplift piles with different slenderness ratios embedded in sand. It is concluded that slenderness ratio is an important factor affecting the ultimate bearing capacity of piles. De Nicola et al. [15] discussed the tensile capacity of uplift piles in sand, and analyzed the key factors affecting the tensile strength with FLAC3D software. The results indicated that Poisson's ratio effect, the friction coefficient of pile-soil interface and the length-diameter ratio were three main factors influencing the tensile strength. By using the three-dimensional finite element method, Al-Baghdadi et al. [16] verified the behavior and mechanical mechanism of screw piles embedded in sandy soil under the vertical and lateral loads. Yan et al. [17] simulated the shear failure effect of piles using the finite element model, and the complex interaction between piles and soil was analyzed. Compared with the existing experimental data, the numerical simulation results of ultimate bearing capacity on pile top had been verified. The numerical simulation also confirmed the theoretical solution. On this basis, it is proposed that the tensile

capacity in sand should be fully considered in the design of uplift piles. Tang et al. [18] also used numerical simulation technology to calculate the pile group effect under the uplift loads. They discussed the influence of length-diameter ratio (L/d), pile spacing-diameter ratio (S_a/d), pile number n and soil type on pile group effect and its coefficient η . Sun et al. [19–21] applied the compatibility condition of pile-soil to establish a three-dimensional finite element model, and analyzed the cooperative work of group pile under vertical loads. On the basis of the failure mode of uplift piles, the side friction, ultimate bearing capacity and Q - s curves, etc. were obtained.

At present, there are many analyses on the deformation response of uplift piles, but the study on cooperative working mechanism of pile groups, the differences of central piles, side piles and corner piles under uplift loads, and the pile-soil plastic changes in ultimate state are still imperfect which need further study. In this paper, FLAC3D software is used to analyze the bearing behaviors of uplift piles, and the deformation and failure characteristics of pile groups are summarized. The results can be used as a reference for the design and construction of uplift piles.

2 Theoretical Analysis on Bearing Failures of Uplift Piles

2.1 The Stress Mechanisms

The uplift piles are pure friction piles without tip resistance, so the side friction is only considered to resist uplift loadings instead of transferring the loads to the deep foundation [22]. When the pile top is subjected to uplift loads, the upward displacement of piles will be resulted relative to the surrounding soil, and the side friction is resistant to the uplift loadings as a whole. The bearing behaviors and failure mechanisms of uplift piles are as follows.

1. Under the influence of axial uplift loads, it appears to be a negative Poisson effect opposite to compressive piles. The pile shrinks inward, so that the radial stress acting on pile side surface is relaxed, which will finally lead to the decrease of the side friction of uplift piles.
2. With the increase of loads, the side friction is functioned gradually from the top to the bottom. For the piles embedded in different depths, the lateral friction does not work at the same time. The larger the uplift load is, the more fully the side friction functions. When the pile tip reaches a critical relative displacement, the side friction resistance is in the ultimate state.
3. Under the axial tension, the pile should not only meet the ultimate bearing capacity standard, but also control the occurrence of cracks widths according to the environmental category and crack control levels. Therefore, developing the prestressing technique of uplift pills is very important.
4. The equal section pile and expanded bottom pile, the short pile and long pile, various embedded geological conditions and soil properties affect greatly on bearing mechanism and failure modes under uplift loads. It is exactly the foundation of establishing the bearing capacity modes.

2.2 The Failure Modes of Equal Section Pile

The theoretical research on uplift piles is mainly focused on ultimate bearing capacity, while it is relatively insufficient about the deformation. For actual project, the criterions to prevent uplift pile failures are mostly based on the maximum allowable deformation, which due to different failure modes. For single equal section pile, the main failure types are as follows [23].

- (1) Cylindrical failure along the interface (Fig. 1a)

For piles with medium-length or longer (the length-diameter ratio, $L/d > 6$), the shear failure surface of soil is cylindrically distributed surrounding the pile. It is the most common damage mode in the actual engineering.

- (2) Inverted frustum shear failure (Fig. 1b)

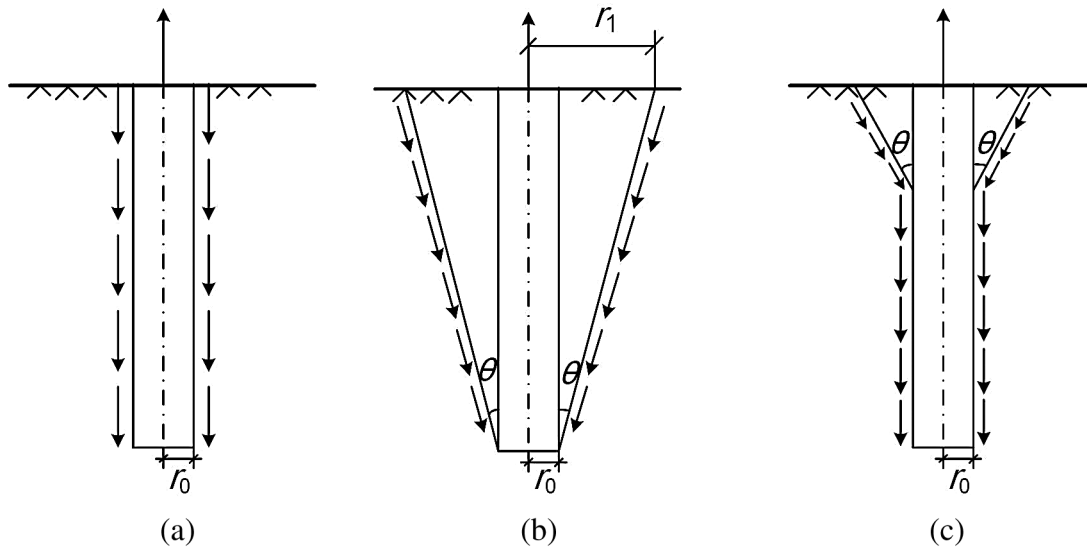


Figure 1: Failure modes on equal section uplift pile

This failure form is mainly concentrated in post grouted bored piles and tubbiness bored piles in gravel or soft rock ($L/d \leq 6$), the weight of inverted cone soil is less than the total side friction resistance of the uplift pile, so that the inverted cone-type destruction will emerge along the whole length.

(3) Composite failure mode

The composite shear failure surface often occurs in bored pile in rigid clays, the side surface of the uplift pile is rugged and the pile-soil interface is highly bonded. There are mainly two shapes of composite failure, reverse frustum shape is at the top and cylindrical shear damage is at below (Fig. 1c).

3 Affecting Factors of Uplift Pile Performance

3.1 Modeling

According to the geologic survey report of a subway station, the FLAC3D software is used to study the bearing behaviors of uplift piles. The length, width and height of the calculation model are 10 m, respectively, and the diameter of the single pile is 1 m. Considering the symmetry of the model, a half model is chosen as the computational domain. Among them, an isotropic elastic model is adopted for uplift piles, and a constitutive model of soil is Mohr-Coulomb model. The piles were modeled as concrete pipes, with a diameter of 0.5 m, giving a bulk modulus of 200 GPa, and shear modulus of 80 GPa. A Mohr-Coulomb soil model was adopted. The soil was modeled as an elastic-perfectly plastic material, with a Mohr-Coulomb strength criterion of $c = 26$ kPa, $\varphi_s = 25^\circ$. The bulk modulus is 67 GPa, and shear modulus is 11.6 GPa. Interfaces between pile and soil had a Mohr-Coulomb strength criterion along the pile side, with $c' = 10.8$ kPa, $\phi = 18^\circ$, and a zero-tension criterion at the pile base [15,23].

The finite element model for calculation is shown in Fig. 2, where the grid division of the uplift pile and the surrounding soil can be identified clearly. According to the soil properties of the site, the calculated soil is simplified as clay, and other critical material properties of the model are shown in Tab. 1.

According to the research purposes, the calculation scheme is divided into three groups including changing the length-diameter ratio (L/d) of uplift piles, the friction angle of soil and the pile types, respectively. The uniform uplift loads are applied on pile top in steps till the pile reaches the ultimate failure state. The variations in displacement and stress along the pile are monitored, and the deformation response and the pile behaviors are analyzed.

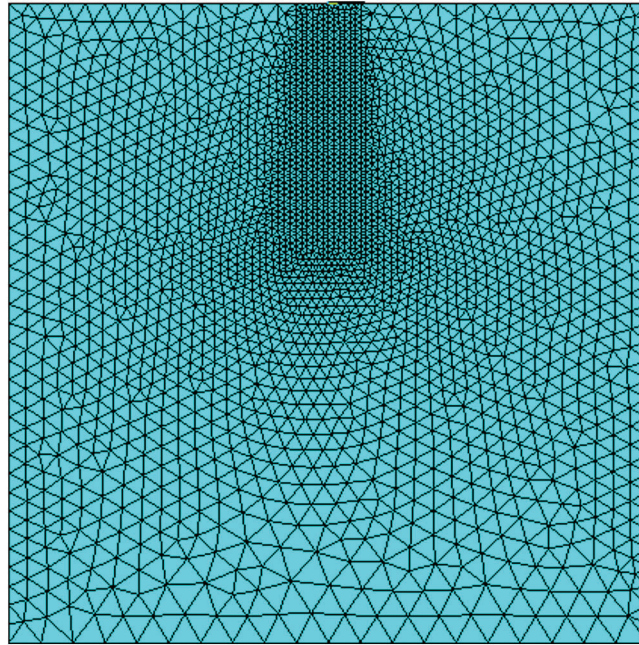


Figure 2: A 3D mesh subdivision graph of the calculation model

Table 1: Physical parameters of the materials

Parameter	Symbol	Value	Unit
Elastic modulus of soil	E_s	23.7	MPa
Elastic modulus of uplift piles	E_P	30,000	MPa
Density of soil	ρ_s	1.84×10^3	kg/m ³
Density of uplift piles	ρ_P	2.8×10^3	kg/m ³
Poisson ratio of uplift piles	ν_P	0.2	—
Fiction angle of soil	φ_s	25	°
Cohesion	C	26.3	kPa

Note: φ_s is the effective internal friction angle in soil derived by consolidated undrained triaxial tests.

3.2 Influence of Length-Diameter Ratio on Uplift Performance of Single Pile

The length-diameter ratio (L/d) is the ratio of length L to diameter d of the uniform section uplift pile, it has a great influence on failure modes and ultimate uplift bearing capacity. The pile length of the model is 1, 1.5, 2, 2.5, 3, 3.5 m, respectively, and the diameter is 0.5 m. Thus, the length-diameter ratio of the uplift piles are 2, 3, 4, 5, 6 and 7, which are numbered A1 to A6 in turn. Fig. 3 shows the load-displacement curves of pile top in loading process. It can be seen clearly that the variation in curves are similar: when the load is small, the slope of the curves change little, showing a “slowly varying” trend, indicated that the uplift pile is undergoing elastic failure. When the load increases to a certain extent, the curve shows an “abruptly increasing” trend. The state corresponding load of the sudden change is the ultimate uplift bearing capacity of the uplift pile [24], indicates that it has undergone the plastic failure.

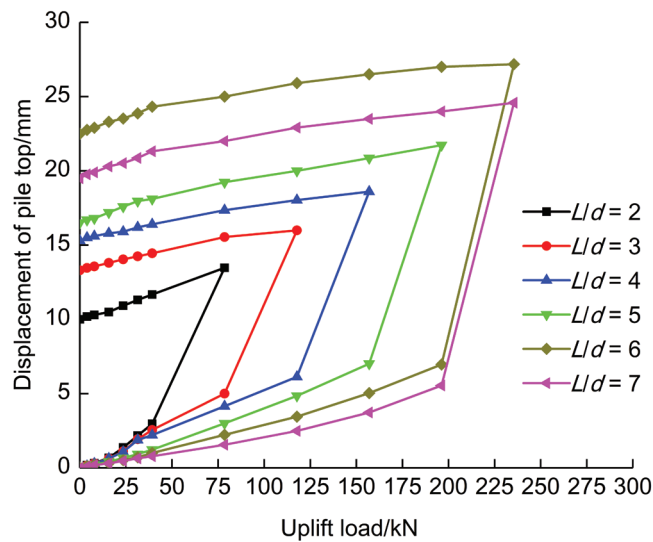


Figure 3: The load-deformation curves of A1 to A6 piles

Unloaded to 0 gradually after the uplift piles reach the ultimate failure state, the pile top displacement decreases step by step, but it cannot return to the original state, which also proves that the plastic deformation has occurred. The final displacement on pile top is called the residual deformation S_r . It is because the pile endures excessive tensile stress applied in the shallow parts, and the cracking deformation affects the durability of the piles.

The length-diameter ratio affects the pile top displacement obviously. When $L/d \leq 6$, the ultimate bearing capacity of single pile increases with the increasing length-diameter ratio, and the displacement of pile top also increases accordingly, which indicates that the uplift pile can resist a great degree of deformation. When $L/d > 6$, the ultimate bearing capacity increases slightly, while the deformation starts to decline gradually.

In summary, increasing of length-diameter ratio, on the one hand, increases the pile weight to resist the uplift loads, and improves the ultimate bearing capacity of uplift piles. On the other hand, the contact area between pile and soil is also enlarged, which increases the side friction. If the pile top reaches the ultimate failure state at the earlier time, the bottom part has a bearing potential, which can make the uplift pile exert greater bearing capacity. The length-diameter ratio can change the failure modes of the pile in a certain range as well. For stub piles, the side resistance is improved by using resist draw cast-in-place piles or post-grouting piles. Thus, as the length-diameter ratio increases, the bearing capacity of single pile gets better, and it is not easy to be failure. However, the bearing capacity cannot be improved by increasing the pile length only. If the stiffness of the uplift pile is low, the pile is easy to be broken while increasing the uplift load to some extent, which should be concerned.

3.3 Influence of Pile-Soil Interface Characteristic on Uplift Behavior

Because the uplift pile is a pure friction pile, the uplift loading is mainly resisted by the lateral friction between pile and soil. For the studies of interfacial sliding and debonding, the friction parameters of contact surface are particularly important relative to the stiffness.

The soil-pile friction angle δ was measured from the direct shear test by using the pile surface material and sand of required compactness [8,25]. According to the research of Potyondy [26,27], the friction angle of pile and soil interface is the key factor affecting the bearing capacity. For clay, it is appropriate that the ratio of δ and φ_s is 0.6 to 0.7. The friction angle in soil is set to be 25° , 30° and 35° , and the piles are numbered B1, A3 and B2, respectively. Fig. 4 shows the influencing curves of friction angle on pile top displacement under the uplift loads, and the interface characteristics of the piles are analyzed.

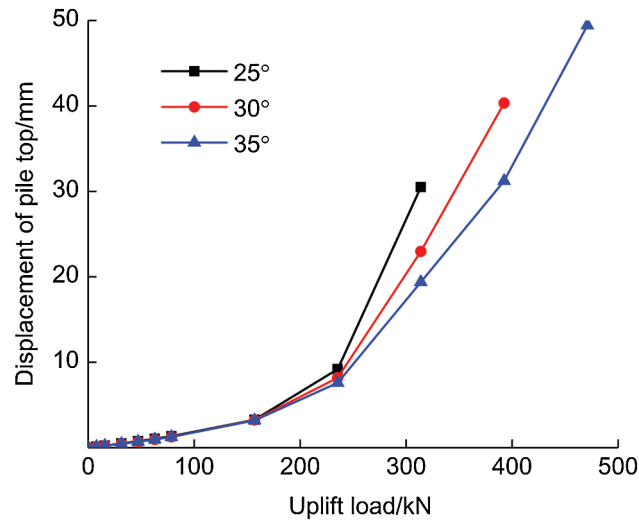


Figure 4: The influencing curve of friction angle to pile top displacement

According to the load-displacement curves of pile top, when the uplift load is small, the displacement of pile top increases slowly, and the slope of the curve remains basically unchanged. The linear trend shows that there is only static friction between pile and soil without relative slip, that is, elastic deformation is occurred at the initial stage of loading. With the increase of loads, the pile reaches the ultimate failure state successively. It can be seen clearly that increasing the internal friction angle φ_s can improve the bearing capacity of uplift piles. The ultimate uplift capacity of B1, A3 and B2 pile is 235.5, 314 and 392.5 kN, respectively. Increasing the soil friction angle means increasing the friction coefficient of pile-soil interface. It is known from the equation $F = \mu N$, when the normal pressure on the pile surface is constant, the larger the friction coefficient is, the greater the side friction resistance is, so that the uplift bearing capacity of uplift piles is improved. The uplift resistance of the shafts increase with the degree of roughness of the pile. In practical engineering, the lateral friction resistance of pile-soil interface changes by adopting the post grouting piles, and the working performance of uplift piles can be enhanced.

3.4 Influence of Pile Type on Uplift Behaviors

In order to study the influence of pile type on bearing capacity, the calculation models of square pile and enlarged end pile are established supplementarily on the basis of single uniform-section model pile, which is numbered A3, C1 and C2, respectively. The length and width of square pile are both 0.5 m. For C2 pile, the upper constant section part remains unchanged, and the diameter D of the expanded head is 1 m. The bearing failure characteristics of three pile types are calculated by numerical simulation software.

Figs. 5–7 show the failure characteristics of soil under the ultimate state when A3, C1 and C2 piles are subjected to the uplift loads. It can be seen clearly that, there are great differences among these three piles. No matter how different the pile types are, the side friction is always gradually exerted from the top to the bottom. The larger the uplift load on the pile top is, the more fully the side friction works. When the uplift pile is in the ultimate failure state, the plastic failure zone of soil around the pile will be in transfixion, and the uplift pile then loses its bearing capacity. After the cylindrical uplift pile reaches the ultimate state, the upper soil is in the shape of inverted conical failure. The soil is subjected to cylindrical shear failure along the pile, which confirms the theoretical failure mode in Section 2.2. A small vacuum space is formed beneath the uplift pile, and the adsorbability of soil is produced, which helps the pile and soil to bear the uplift loads together. The lateral friction resistance is relatively small in the middle of square uplift pile. If the uplift load increases continuously, there is no adsorption force at the end, which is only relied on the upper parts of the pile to bear the load. When the enlarged end of C2 pile moves up, the shear failure surfaces in different directions will occur in the foundation soil, and the failure mode becomes complex.

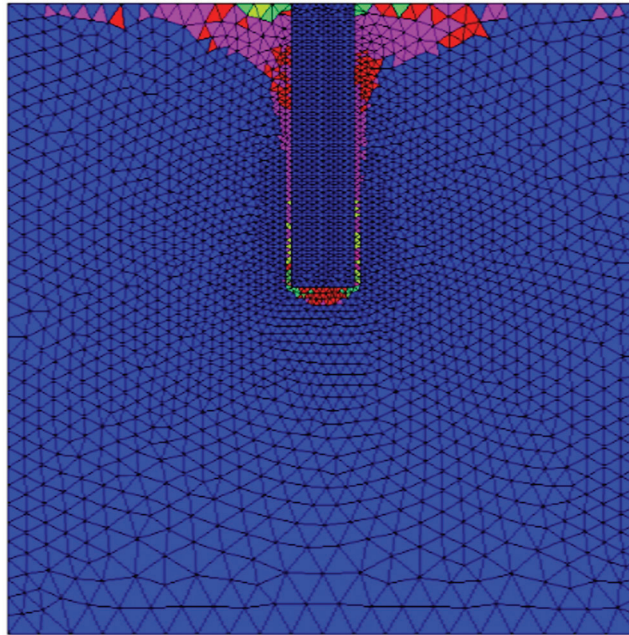


Figure 5: The failure state of soil around the cylindrical pile

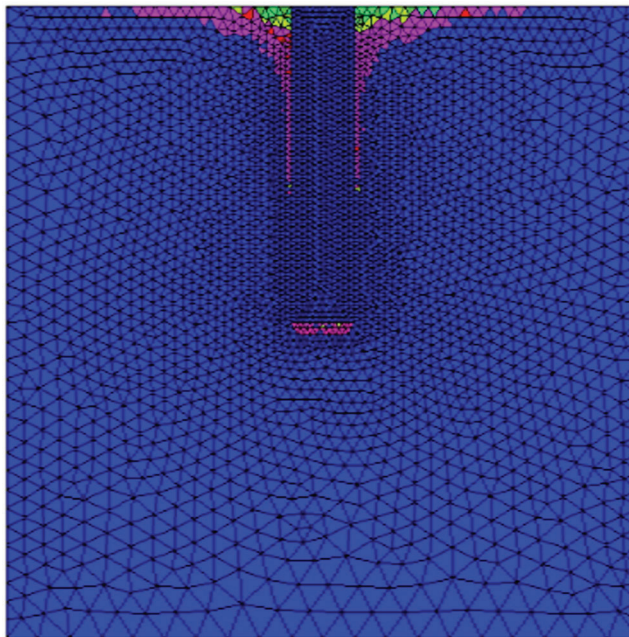


Figure 6: The failure state of soil around the square pile

Above all, the uplift performance of enlarged end pile is superior to the equal section cylindrical pile and the square pile. When the relative displacement occurred between the uplift pile and the surrounding soil, the soil above the enlarged head has a barrier effect on pile deformation, causing the soil within the influencing range to resist the uplift loads. Thus, the side resistance of uplift pile is significantly enhanced, and a large plastic failure zone is formed. Considering saving the costs, the spherical end can be simplified appropriately: retain the upper part of the sphere at the position of diameter, a truncated cone expander is formed, which also has high side friction.

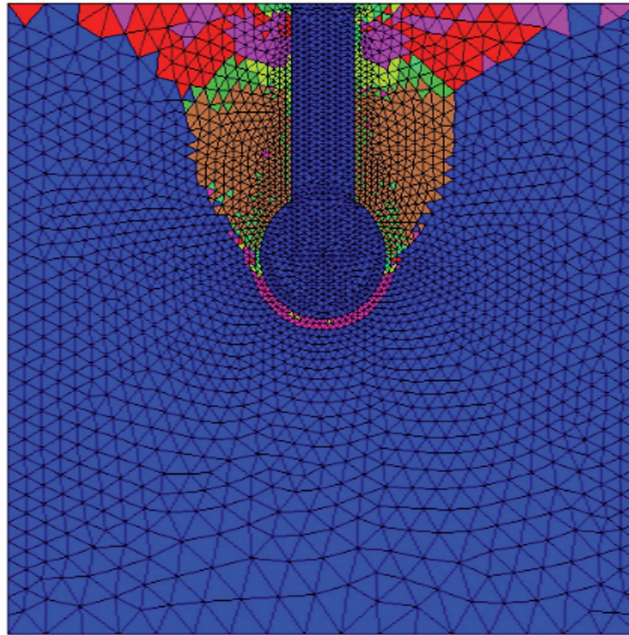


Figure 7: The failure state of soil around the enlarged end pile

4 Cooperative Work Characteristics of Uplift Pile Group

In this chapter, the cooperative working characteristics of uplift pile group are obtained by numerical simulation technology. Analyze the pile top displacement and stress along the center piles, side piles and corner piles, try to find the position where the uplift bearing capacity is relatively small, and finally optimize the designing scheme on the basis of the actual project.

4.1 Modeling and Excavation

The calculation model is established including 21 equal section uplift piles with a length-diameter ratio of 5, a 25 m deep foundation and a diaphragm wall with a thickness of 1 m. The distance between the adjacent piles is 10 m. Because the distribution of uplift piles is symmetrical, one fourth of the model is taken as the calculation domain. The layout of the piles is shown in Fig. 8, where No. 1, 2 and 3 are center piles, Nos. 4, 5, 6 and 7 are side piles, and Nos. 8 is corner pile. A 3D calculation model is obtained by FLAC3D software, which is shown in Fig. 9. In order to meet the design standard, groundwater is set in the whole underground space, and a rising trend of the structure will be produced with buoyance.

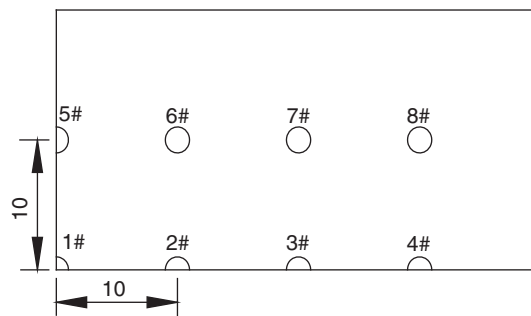


Figure 8: The layout of group piles

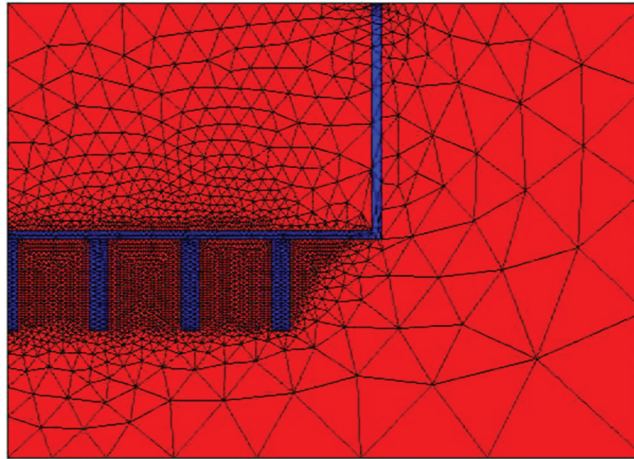


Figure 9: The mesh drawing of calculation model

The foundation pit is excavated in five times, and dig 5 m each time. Because the uplift piles are set before the excavation, the foundation pit unloading will obviously change the stress field and displacement field of the surrounding soil, which will certainly have a negative effect on the deformation of group piles. During the excavation period, the uplift piles are mainly affected from three aspects: (1) the soil around the piles appears to arch upward, causing an adverse effects of pit resilience on uneven settlement and mechanical characteristics of the structures. (2) Relative slip occurs at the pile-soil interface, which results in an initial lateral friction between piles and soil. Thus, the uplift piles will passively lost the bearing capacity at the beginning, which has an obvious influence on the behavior of uplift piles. (3) The stress field of pile groups has changed. The normal stress k_n at pile-soil interface is reduced as well as the net ultimate bearing capacity of uplift piles [28,29].

Monitor the displacement and stress of uplift piles and the surrounding soil successively during the excavation, and the displacement of pile top is shown in Tab. 2.

Table 2: The variation in pile top displacement during the excavation (unit: mm)

	1	2	3	4	5	6	7	8
Step 1	22.35	22.17	21.33	19.71	20.73	20.67	20.16	19.15
Step 2	49.28	48.91	46.73	41.90	44.47	44.40	43.15	40.11
Step 3	76.15	75.66	72.21	63.61	67.46	67.5	65.61	60.19
Step 4	109.90	109.10	103.60	89.74	96.09	96.15	93.12	84.31
Step 5	143.20	142.00	134.20	115.10	124.80	124.60	120.20	107.90

4.2 The Cooperative Work Effect

As a result, the deformation differences of center piles, side piles and corner piles are also compared clearly. Export the vertical displacement nephogram of the calculation model, and the variation in group piles at different positions can be obtained directly, which is shown in Fig. 10.

As is vividly shown in the picture, the largest deformation of uplift piles is the center pile, the side pile is the next, and the corner pile is the smallest. This is because the uplift piles suffer different restraints from the surrounding soil. The central pile locates in the center of the pile group, and the soil-squeezing action around the pile is the greatest, causing the normal stress in soil uneasy to diffuse. Therefore, the center pile and soil

cooperative work effect is the greatest [9,22]. The difference of normal stress directly leads to the variations in friction resistance of uplift piles, among which the central pile is the largest, so it deforms and reaches the limit failure state the earliest during the loading period. When the center pile cannot continue to bear the loads, the normal stress transfers to side pile and corner pile in turn. The load is redistributed within the pile group, and the side pile and corner pile also reach the limit condition gradually. On the contrary, the corner pile locates at the edge of pile group foundation, which is disturbed minimally by the soil around the pile. The stress diffusion effect is the most obvious, and the lateral friction is exerted the most significantly.

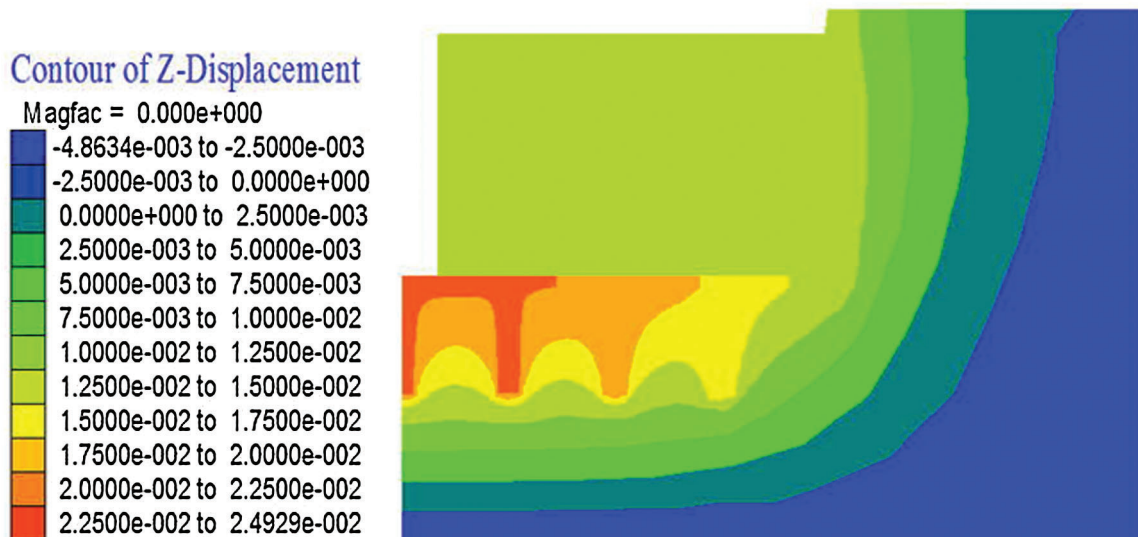


Figure 10: The vertical displacement nephogram of group piles after the excavation

The uplift bearing capacity of pile groups can be summarized as follows. The largest is corner pile, the side pile is the next, and the center pile is the smallest. According to the results, the weakest position of bearing the load is found in the group pile, and the corresponding measures can be taken to improve the ultimate bearing capacity.

4.3 Scheme Optimization in the Engineering

In order to study the overall anti-floating characteristics of the subway tunnels and put forward better control measures. Combining with the aforementioned results, the ultimate bearing capacity of center pile is the smallest, which is necessary to be enhanced. Therefore, an equal section pile is redesigned as the enlarged end pile, and the layout of pile groups is shown in Fig. 11a, the uplift piles are shown in Fig. 11b. Excavate the foundation pit in accordance with the formal steps, the displacement nephogram of piles is obtained, as shown in Fig. 12. Compared with Fig. 10, it's clear that the enlarged end uplift pile can increase the bearing capacity of center pile in the affected range.

The statistical results of pile top displacement in two cases are shown in Tab. 3. It is indicated that the main underground structure of the subway tunnel has a trend of float. When all the uplift piles are of the equal section, the deformation range of the piles is between 2.46 cm to 2.98 cm. When the No. 2 pile is changed into expanded end, the deformation of uplift piles is in a range of 2.14 cm to 2.48 cm. The results show that, changing the pile types from equal section to enlarged end at the key position can significantly enhance the bearing capacity. Therefore, it is suggested to space the enlarged end piles and equal section piles along the central axis of the principal part of the project. In the calculation model, the No. 2 belled pile can obviously

improve the bearing capacity of all center piles, especially for pile No. 3. However, the enlarged end will loosen the upper soil when subjected to uplift loads, which induces the lateral friction of short piles, and the adverse influence expands with the belled pile numbers. As a result, an arrangement ratio of 1:2 is a proper choice.

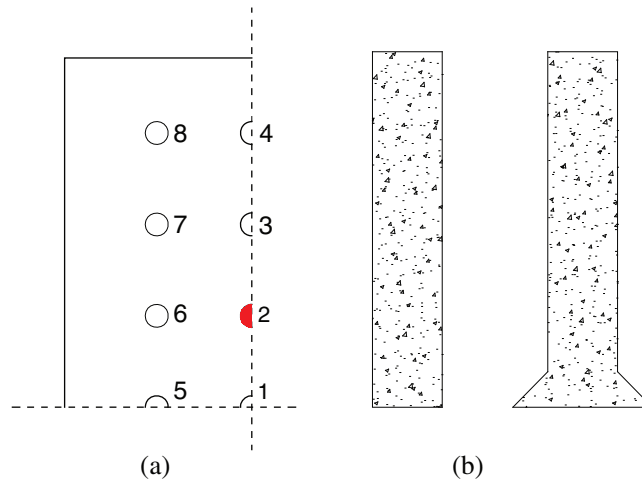


Figure 11: The optimum design plan. (a) The distribution diagram of pile group and (b) The schematic diagram of uplift piles

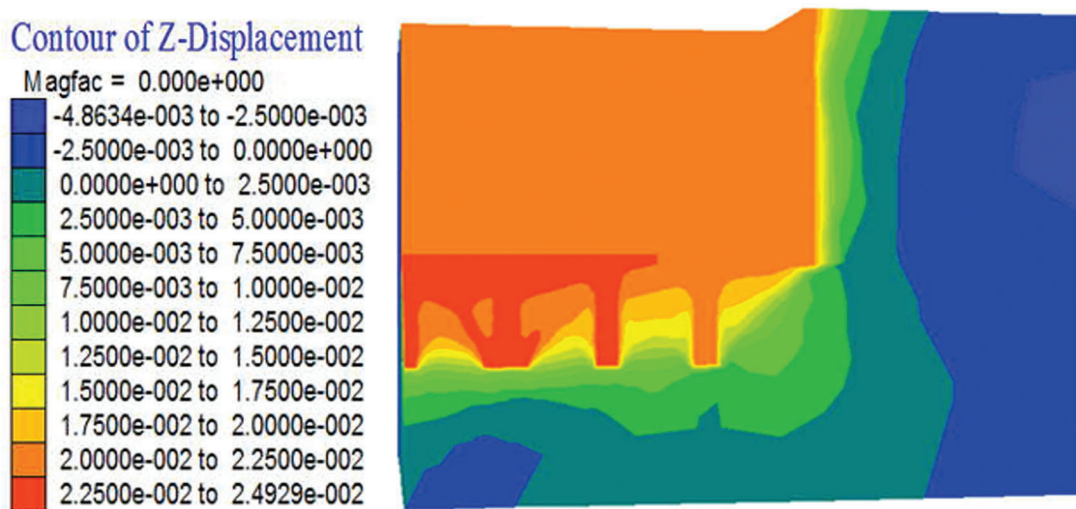


Figure 12: The displacement nephogram of pile top

Table 3: The comparison of the pile top displacement between two cases (unit: mm)

	1#	2#	3#	4#	5#	6#	7#	8#
Case 1	29.81	29.41	27.70	25.24	26.72	26.56	25.72	24.59
Case 2	24.81	24.62	23.38	21.81	22.67	22.60	22.05	21.40

5 Discussion

The bearing failure mechanism of uplift piles is analyzed not only through the deformation response of pile top, but also through the axial force distribution and side friction resistance. The axial force distribution along the pile is one of the important factors studying the load transfer behaviors of uplift piles, and it's also the basis of calculating the side friction. Taking the length-diameter ratio as an example, the distribution curves of axial force of A3, A4 and A5 piles under the loads are obtained, the results are shown in Fig. 13a. As we can see in the picture, increasing the length-diameter ratio, the axial force is improved so that the bearing capacity of the uplift pile is effectively enhanced. The axial force N decreases step by step along the pile, and the axial force increment under the adjacent loads decreases with the depth. On the upper part of the pile, the slope of axial force curve is relatively large, indicating that the axial force changes greatly, while it changes insignificantly at the lower part. The axial force at pile end is always zero, suggesting that the uplift pile is a pure friction pile.

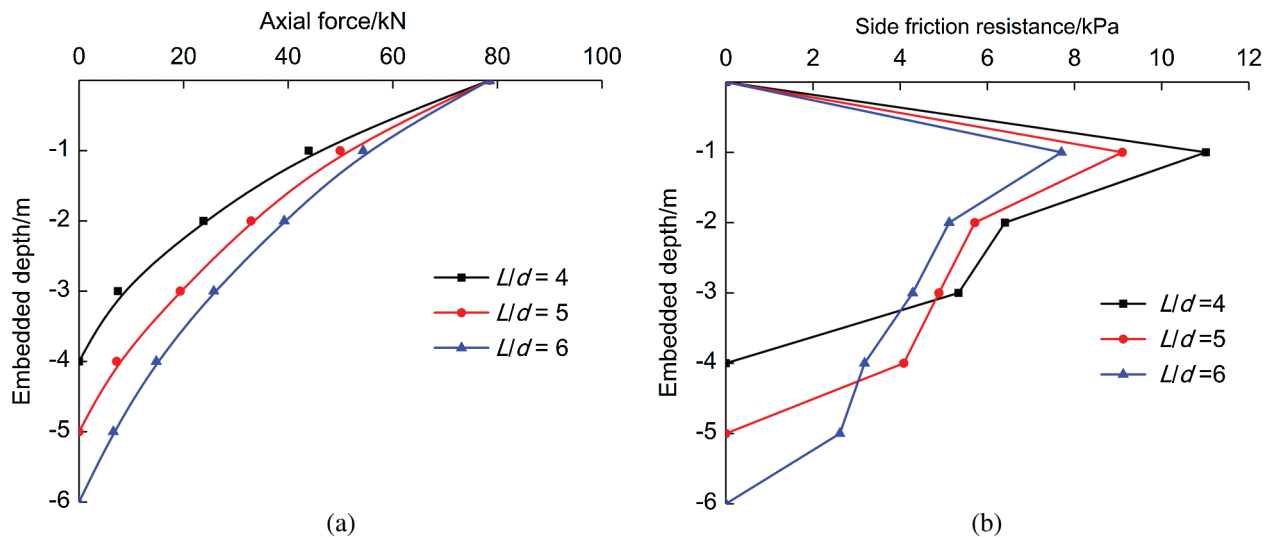


Figure 13: Mechanical analysis of A3 to A5 piles under the same load. (a) The curves of axial force with different length-diameter ratios and (b) The curves of side friction resistance with different length-diameter ratios

Based on the results of axial force, the side friction can be calculated. The formula is as follows

$$\pi d L_i f_{si} = N_{i+1} - N_i \quad (1)$$

where, d is the diameter of the uplift pile, L_i is the pile length of each piece, f_{si} is the side friction resistance of each pile piece, N_{i+1} , N_i is the axial force at pile top and bottom of each piece.

The uplift load is transferred to the surrounding soil through the lateral friction resistance f_s . With the increasing load, the lateral friction resistance is mobilized gradually [30,31]. The distribution of side friction with different length-diameter ratios can be obtained by Eq. (1), and the curves of side friction along the embedded depth are shown in Fig. 13b. Compared with A3, A4 and A5 piles, the trend of three lateral friction curves are basically the same, which still shows the characteristics of two small ends and a large middle part. When the load is low, the side friction resistance at pile end is almost zero. In the same depth, the larger the uplift load, the greater the side friction is. The lateral friction in pile-soil surface does not work at the same time: after the upper side friction reaches to the limit, it tends to be stable, and then the lower part of soil gradually works. With the continuous increasing load, the soil around the pile

moves upward with the uplift pile, and a vacuum cavity is formed at the pile end. The surrounding soil fills the space, which will eventually lead to the decrease of side friction.

Among the three curves in Fig. 13b, the lateral resistance of A3 pile shapes “short and fat”, while A5 pile curve shapes “high and thin”. From Eq. (1), the uplift load on pile top is approximately equal to the product of the pile perimeter and the area enclosed by the lateral friction curve with the embedded depth axis. If the perimeters are all the same, the curves will show such changing law [32]. In addition, Poisson effect, shear dilatancy and dilatation of soil can also affect the lateral friction resistance of uplift piles, which are not mentioned here.

Besides, the ultimate capacity of uplift piles can also be obtained by combining with the curves of axial force and side friction resistance. Taking A3 pile as an example, the mechanical analysis along the pile are shown clearly in Fig. 14 during all levels loading action.

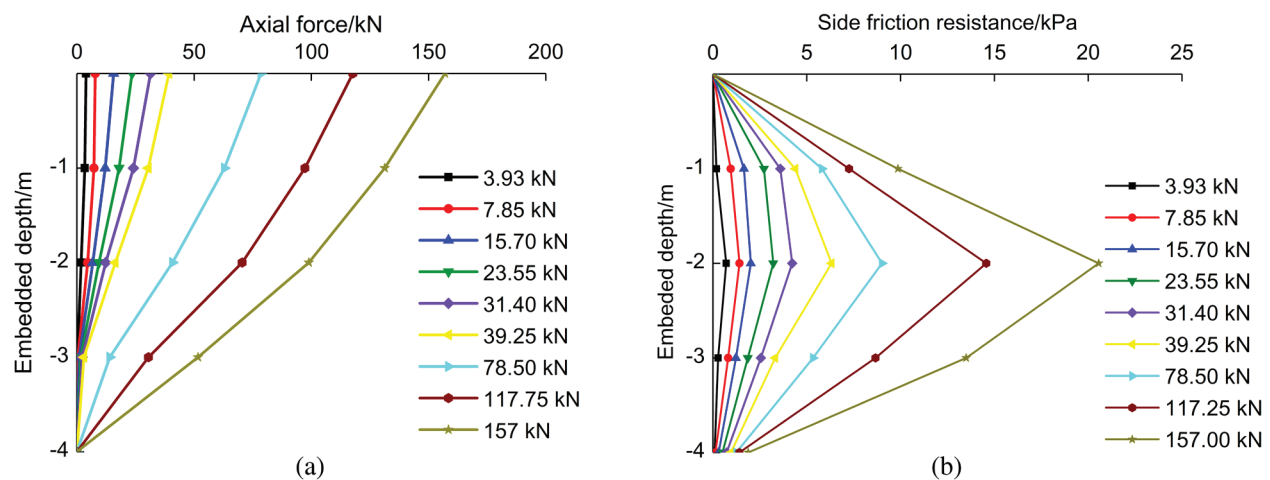


Figure 14: Mechanical analysis of A3 pile under different loads. (a) The axial force distribution curves of A3 pile and (b) The side friction resistance curves of A3 pile

The variation trend of the curves in Fig. 14 are basically similar as Fig. 13 showing the characteristics of pure friction pile. In Fig. 14a, the axial force N decreases step by step with the increase of embedded depth, and the slope of axial force in lower part gradually changing with the increasing load. When the uplift load is small, the axial force does not have an obvious impact on bearing capacity. The slope of the curves at the upper part change little until the uplift load is up to 117.75 kN, which is indicated that the uplift pile has reached the ultimate bearing condition. In Fig. 14b, the lateral friction is generally characterized by small ends and large middle part, and the side friction resistance at pile end is nearly zero. With the increase of the uplift loads, the side friction resistance change rapidly and the slope of the curves remains steady, which is indicated that the pile is gradually in plastic destruction state. Combined with the results in Section 3.2, the ultimate lateral friction of A3 pile is 20.56 kPa.

6 Conclusions

In this paper, numerical simulation technology is used to study the effect of length-diameter ratio, pile-soil interface characteristics and pile type on the bearing behaviors of single uplift pile. The methods to improve the ultimate bearing capacity are summarized, and the cooperative work between pile and soil is analyzed to optimize the design of pile group in practical engineering. The conclusions are as follows.

1. The length-diameter ratio (L/d) has an obvious influence on the failure mode and the contact area of pile and soil interface. In a certain range, increasing length-diameter ratio makes the lateral friction

work more efficiently, and the bearing capacity of uplift pile gets better. If increasing the pile length only, a risk of breaking the piles will occur under higher uplift loads, which will increase the costs and affect the structural safety as well. For stub pile ($L/d < 6$), the side resistance can be improved by applying resist draw cast-in-place piles or post-grouting piles.

2. For the occasion of interfacial sliding and debonding between pile and soil, the friction angle of contact surface has a significant influence. Increasing the friction angle of the soil is equivalent to increasing the roughness of the pile-soil interface. Because the uplift pile is a pure friction pile, which is only relied on the lateral friction to resist the uplift load. The larger the roughness of pile-soil interface, the greater the side friction resistance is, and the uplift bearing capacity is much greater.
3. The pile type has an obvious effect on bearing capacity of uplift piles. Comparing with the equal section cylindrical pile, square pile and expanded end pile, it is indicated that the expanded end uplift pile has a better uplift performance than other types. When the relative displacement occurs between the pile and the surrounding soil, the soil above the enlarged head has a certain barrier effect on pile deformation, resulting in enhancing the side friction resistance significantly.
4. Because the central pile, side pile and corner pile are constrained differently in pile groups, the cooperative work effect between pile and soil is different. The uplift bearing capacity of pile groups is summarized as the largest corner pile, the side pile is the next, and the center pile is the smallest. According to the results, the pile type of center pile at the axis is changed into enlarged end pile, which will improve the bearing capacity pertinently with less costs.

Funding Statement: This work was supported by National Key Research, Development Project of China (2016YFC0802206), Disaster Prevention and Mitigation Collaborative Innovation Center for Large Infrastructure of Hebei Province (2017), and Postgraduate Innovative Funding Projects of Hebei Province (CXZZSS2018060).

Conflicts of Interest: The authors declare that they have no conflicts of interest to report regarding the present study.

References

1. Wang, Y. Q., Zhang, L. (2006). Research on bearing capacity behavior of uplift pile. *Journal of Harbin Institute of Technology*, 38(3), 389–391 (in Chinese).
2. Chattopadhyay, B. C., Pise, P. J. (1986). Uplift capacity of piles in sand. *Journal of Geotechnical Engineering*, 112(9), 888–904. DOI 10.1061/(ASCE)0733-9410(1986)112:9(888).
3. Zhang, Q. Q., Li, S. C., Zhang, Q., Li, L. P., Zhang, B. (2015). Analysis on response of a single pile subjected to tension load using a softening model and a hyperbolic model. *Marine Georesources & Geotechnology*, 33(2), 167–176. DOI 10.1080/1064119X.2013.828822.
4. Alawneh, A. S. (2005). Modelling load–displacement response of driven piles in cohesionless soils under tensile loading. *Computers and Geotechnics*, 32(8), 578–586. DOI 10.1016/j.compgeo.2005.11.003.
5. Chen, X. Q., Zhao, C. F., Gan, A. M. (2009). Study on model test of uplift and compression piles in layered soil. *Chinese Journal of Underground Space and Engineering*, 5(S2), 1537–1541 (in Chinese).
6. Chen, X. Q., Zhao, C. F., Gan, A. M. (2011). Study of model test of uplift and compression piles in sand. *Rock and Soil Mechanics*, 32(3), 738–744 (in Chinese).
7. Das, B. M. (1983). A Procedure for estimation of uplift capacity of rough piles. *Soils and Foundations*, 23(3), 122–126. DOI 10.3208/sandf1972.23.3_122.
8. Dash, B. K., Pise, P. J. (2003). Effect of compressive load on uplift capacity of model piles. *Journal of Geotechnical and Geoenvironmental Engineering*, 129(11), 987–992. DOI 10.1061/(ASCE)1090-0241(2003)129:11(987).
9. Gaaver, K. E. (2013). Uplift capacity of single piles and pile groups embedded in cohesionless soil. *Alexandria Engineering Journal*, 52(3), 365–372. DOI 10.1016/j.aej.2013.01.003.

10. Madhusudan Reddy, K., Ayothiraman, R. (2015). Experimental studies on behavior of single pile under combined uplift and lateral loading. *Journal of Geotechnical and Geoenvironmental Engineering*, 141(7), 04015030. DOI 10.1061/(ASCE)GT.1943-5606.0001314.
11. Eswar, P., Naga, S. T., Patra, N. R. (2008). Effect of compressive load on uplift capacity of single piles: an investigation. *GeoCongress*, New Orleans.
12. Faizi, K., Armaghani, D. J., Sohaei, H., Rashid, A. S. A., Nazir, R. (2015). Deformation model of sand around short piles under pullout test. *Measurement*, 63, 110–119. DOI 10.1016/j.measurement.2014.11.028.
13. Faizi, K., Kalatehjari, R., Nazir, R., Rashid, A. S. A. (2015). Determination of pile failure mechanism under pullout test in loose sand. *Journal of Central South University*, 22(4), 1490–1501. DOI 10.1007/s11771-015-2666-8.
14. Faizi, K., Rashid, A. S. A., Armaghani, D. J., Nazir, R., Momeni, E. (2017). The influence of bituminous coating on uplift resistance of short pile foundations in sand. *Soil Mechanics and Foundation Engineering*, 54(3), 177–182. DOI 10.1007/s11204-017-9454-4.
15. De Nicola, A., Randolph, M. F. (1993). Tensile and compressive shaft capacity of piles in sand. *Journal of Geotechnical Engineering*, 119(12), 1952–1973. DOI 10.1061/(ASCE)0733-9410(1993)119:12(1952).
16. Al-Baghdadi, T. A., Brown, M. J., Knappett, J. A., Al-Defae, A. H. (2017). Effects of vertical loading on lateral screw pile performance. *Proceedings of the Institution of Civil Engineers-Geotechnical Engineering*, 170(3), 259–272. DOI 10.1680/jgeen.16.00114.
17. Yan, W. J., Gao, F. P. (2010). Numerical analysis of interfacial shear degradation effects on axial uplift bearing capacity of a tension pile. *Procedia Engineering*, 4, 273–281. DOI 10.1016/j.proeng.2010.08.031.
18. Tang, B., Chen, X. P. (2005). Finite element analysis of effect of pile group. *Rock and Soil Mechanics*, 26(2), 299–302 (in Chinese).
19. Sun, X. L., Mo, H. H. (2009). An analytical calculation method for displacement of under-reamed tension piles. *Chinese Journal of Rock Mechanics and Engineering*, 28(1), 3008–3014 (in Chinese).
20. Sun, X. L., Yang, M. (2008). Analysis of nonlinear deformation of uplift piles by modified method of deformation compatibility. *Chinese Journal of Rock Mechanics and Engineering*, 27(6), 1270–1277 (in Chinese).
21. Sun, X. L., Yang, M., Mo, H. H. (2008). Displacement of base-enlarged tension piles calculated by load transfer method. *Chinese Journal of Geotechnical Engineering*, 30(12), 1815–1820 (in Chinese).
22. Liu, J. L. (2004). Group effects and some problems on the concept design of pile group foundation under vertical load. *China Civil Engineering Journal*, 37(1), 78–83 (in Chinese).
23. Liu, J. L., Gao, W. S., Qiu, M. B. (2010). *Application manual of technical specification for building pile foundation*. China Architecture & Building Press (in Chinese).
24. Huang, G. L., Fang, Q., Su, R. Z. (2010). Field test on uplift behavior of micropiles in soft ground. *Chinese Journal of Geotechnical Engineering*, 32(11), 1788–1793 (in Chinese).
25. Zhang, Q. Q., Li, S. C., Li, L. P. (2015). Field and theoretical analysis on the response of destructive pile subjected to tension load. *Marine Georesources & Geotechnology*, 33(1), 12–22. DOI 10.1080/1064119X.2013.764558.
26. Potyondy, D. O. (2007). Simulating stress corrosion with a bonded-particle model for rock. *International Journal of Rock Mechanics and Mining Sciences*, 44(5), 677–691. DOI 10.1016/j.ijrmms.2006.10.002.
27. Potyondy, D. O. (2015). The bonded-particle model as a tool for rock mechanics research and application: current trends and future directions. *Geosystem Engineering*, 18(1), 1–28. DOI 10.1080/12269328.2014.998346.
28. Chen, J. J., Wang, J. H., Fan, Q., Wang, W. D. (2009). Behavior of up-lift pile foundation during large-scale deep excavation. *Chinese Journal of Geotechnical Engineering*, 31(3), 402–407 (in Chinese).
29. Wei, L. Y., Qin, S. W., Chen, H. E. (2014). Analysis on rebounding displacement of single pile and pile group under excavation. *Journal of Jilin University (Earth Science Edition)*, 44(2), 584–590 (in Chinese).
30. Li, G. X., Huang, F., Shuai, Z. J. (1999). Test study of influence of loading ways on friction of piles. *Industrial Construction*, 29(12), 19–21 (in Chinese).
31. Zhang, Z. M., He, Y. J., Zou, J. (2010). Experimental study of behavior comparison of grouted and non-grouted uplift piles in soft soil. *Chinese Journal of Rock Mechanics and Engineering*, 29(12), 2566–2572 (in Chinese).
32. Lian, X. H. (2013). *The analysis on bearing capacity of uplift pile foundation (M.S. Thesis)*. Harbin Institute of Technology, Harbin (in Chinese).